Chytrid infecting the bloom-forming marine diatom Skeletonema sp.:

Garvetto, Andrea; Badis, Yacine; Perrineau, Marie-mathilde; Rad-menéndez, Cecilia; Bresnan, Eileen; Gachon, Claire M.m.

Published in:
Fungal Biology

Publication date:
2019

Chytrid infecting the bloom-forming marine diatom *Skeletonema* sp.: morphology, phylogeny and distribution of a novel species within the Rhizophydiales

Andrea Garvetto[1], Yacine Badis[1], Marie-Mathilde Perrineau[1], Cecilia Rad-Menéndez[2], Eileen Bresnan[3], Claire M. M. Gachon[1]

[1] Scottish Association for Marine Science, Scottish Marine Institute, Oban, UK.

[2] Culture Collection of Algae and Protozoa, Scottish Association for Marine Science, Scottish Marine Institute, Oban, UK

[3] Marine Scotland Science, Marine Laboratory, Aberdeen, UK

Abstract

Chytrids have long been recognised as important parasites of microalgae in freshwater systems, able to shape the dynamics of blooms, the ~~genetic structure~~gene pool of their host and phytoplankton succession. In the sea however, where the presence of these organisms is erratic and ephemeral, studies concerning chytrids are sparse and confined to metabarcoding surveys or microscopy observations. Despite the scarcity of data, chytrid epidemics are supposed to play an important role in marine biogeochemical cycles, being one of the drivers of phytoplankton dynamics. Here we combine microscopy observations and *in silico* mining of a single-cell whole genome to molecularly and morphologically characterise a novel chytrid parasite of the dominant diatom genus *Skeletonema*. Morphological observations highlight features of the thallus and ascertain the parasitic nature of the interaction whilst the genetic markers obtained allows for a phylogenetic reconstruction, placing the new species in the order Rhizophydiales. Thanks to the molecular data obtained we are also able to provide a first investigation of the global distribution of this organism by screening the Ocean Sampling Day (OSD) dataset, highlighting a northern transatlantic dissemination.

Keywords

Marine microbial diversity, marine fungi, plankton parasites, single-cell analysis, NGS

1. Introduction

Zoosporic true fungi belonging to the early diverged phylum Chytridiomycota (Hibbett *et al.*, 2007) are widespread microorganisms known to dominate the fungal community in freshwater ecosystems (Monchy *et al.*, 2011; Jobard *et al.*, 2012) where they play an important role as parasites and saprobes (Gleason *et al.*, 2008; Frenken *et al.*, 2017). Parasitic associations of chytrids with microalgae have long been known in lentic systems (Canter and Lund, 1953; Sparrow, 1960), where chytrid propagules act as an important ~~career~~ carrier of fixed carbon from inedible algae to grazing zooplankters by means of the mycoloop (Kagami *et al.*, 2014); and are suspected to be one of the main drivers maintaining the genetic diversity of their algal hosts through highly host-specific associations (Ibelings *et al.*, 2004; De Bruin *et al.*, 2008; Gsell *et al.*, 2013). Despite the prevalence of studies targeting lakes, chytrids have been recorded as a major component of the microbial community in various ecosystems by means of molecular surveys, especially in extreme habitats such as alpine snow (Naff *et al.*, 2013), sea-ice (Hassett *et al.*, 2017), high elevation soils (Freeman *et al.*, 2009) and marine hydrothermal vents (Le Calvez *et al.*, 2009). Whenever these habitats allow for the survival of photosynthetic organisms, the co-occurrence (Freeman *et al.*, 2009; Naff *et al.*, 2013; Brown *et al.*, 2015) or parasitic association (Hassett and Gradinger, 2016; Hassett *et al.*, 2017) between phototrophs and chytrids has been reported. In the sea, recent metabarcoding surveys unveiled an unexpectedly large and undescribed biodiversity within the Chytridiomycota (Comeau *et al.*, 2016; Hassett and Gradinger, 2016; Hassett *et al.*, 2017). Despite not being the yearlong dominant fungal taxon (Picard, 2017), a high abundance of chytrids in the plankton was often recorded in short time windows matching coastal blooms of phytoplankters such as diatoms (Taylor and Cunliffe, 2016). In less productive marine ecosystems, such as open ocean oligotrophic gyres, chytrids have been found parasitising dominant photosynthetic picoeukaryotes within the families

Chrysophyceae and Prymnesiophyceae (Lepère *et al.*, 2016). Even if culturing remains a paramount step to fully appreciate and understand the biology of these organisms, establishing and maintaining a dual culture of the parasite and its host (i.e. pathosystem) in the laboratory is challenging (Rad-Menéndez *et al.*, 2018). The isolation of chytrids is further complicated by the erratic and ephemeral presence of these "dazzling and elusive creatures" in the field (Sparrow, 1958). Therefore, most of the information on chytrid ecological role and diversity is underpinned by either sparse microscopic observations that are informative regarding the parasitic interaction but often lack taxonomic resolution; or by broad molecular surveys; which provide sequencing data and an overview of chytrid phylogenetic diversity, but can only be suggestive in terms of ecological function. For these reasons, a big part of chytrid diversity is assigned to the undescribed, uncultivated and functionally uncharacterised dark matter fungi (Grossart *et al.*, 2016), hindering the appreciation of their role in ecosystem dynamics and global biogeochemical cycles.

Diatoms within the genus *Skeletonema* are among the main contributors to planktonic primary productivity in coastal temperate areas worldwide, often representing the dominant diatom during the spring bloom (Borkman and Smayda, 2009; Canesi and Rynearson, 2016). This diatom genus often constitutes the basis of food webs (Bergkvist *et al.*, 2012) and can account for up to 99% of the microphytoplankton community during seasonal blooms (Canesi and Rynearson, 2016). Whilst the contribution and effects of zooplankton grazing has been extensively studied (Bergkvist *et al.*, 2012; Amato *et al.*, 2018), only one study reports chytrids infecting *Skeletonema*, addressing their role in bloom dynamics and phytoplankton species succession off the Chilean coast (Gutiérrez *et al.*, 2016). Here, using a ~~simple~~ method that combines microscopy and single-cell whole genome amplification, we identify a novel chytrid species infecting *Skeletonema* sp. from the west coast of Scotland. We provide a morphological description, molecular identification and a phylogenetic placement for this chytrid within the Rhizophydiales. Finally, thanks to the obtained molecular data, we use the OSD worldwide metabarcoding database (Kopf *et al.*, 2015) to investigate the global distribution of this new species.

2. Methods

2.1 Isolation of the biological material

Plankton samples were collected on the 25th of April 2016 off the pontoon of the Scottish Association for Marine Science (56°27'12.6"N 5°26'12.2"W, Oban, UK) and screened in plastic Petri dishes (145 mm diameter, Greiner Bio One) with a Zeiss IDO3 microscope (32X magnification). *Skeletonema* chains carrying chytrid sporangia were isolated by mouth pipetting. Infected chains were transferred into droplets (~ 5 µL) of fresh f/2+Si medium into 50 mm glass bottom Petri dishes for microscopy observations. Cultivation ~~of the chytrid parasitoid~~ was attempted by ~~inoculating~~ baiting the chytrid parasitoid from environmental samples with *Skeletonema spp.* strains CCAP 1077/1B, CCAP 1077/1C, CCAP 1077/3, CCAP 1077/4, CCAP 1077/5 and CCAP 1077/7 (maintained in f/2+Si) ~~with infected environmental samples~~. None resulted in a successful infection.

2.2 Microscopy

Subsamples containing infected cells were treated with the stains Calcofluor White (CW, Fluka), Wheat Germ Agglutinin Fluorescein isothiocyanate (WGA-FITC, Vector Labs) and Nile Red (NR, Sigma Aldrich). Subsamples of 10 mL were incubated in 100X diluted stain stock solutions (final concentrations: 5 µg mL^{-1} for WGA-FITC or CW; 1 µg mL^{-1} for NR) for 15-30 minutes at room temperature in the dark. After incubation samples were either screened directly in glass-bottom Petri dishes or transferred onto microscopy slides. Observations were carried out at a 100X magnification with a Zeiss LSM 510 microscope (equipped with an AxioCam HRC) in bright field and ~~UV light~~epifluorescence, using an excitation wavelength of either ~ 488 nm (WGA-FITC and NR) or ~ 360 nm (CW). Unstained infected chains were observed in bright field on glass bottom Petri dishes before being isolated singularly for downstream molecular analysis.

2.3 DNA amplification and sequencing

Single infected chains were transferred by mouth pipetting into 1.5 mL sterile Eppendorf tubes. Care was taken to sterilise the glass tip of the mouth pipette with boiling freshwater before each

isolation. Isolated single chains were frozen at -20 ˚C for at least 12 hours before being thawed and subjected to multiple displacement whole genome amplification (MDA; Lasken, 2007) with the Qiagen REPLI-g® Single Cell Kit, as per the manufacturer's instruction. Amplified material was stored at -80 ˚C and aliquots- were diluted 100 times in autoclaved Milli-Q water before downstream PCR amplifications. PCRs were performed in a total reaction volume of 50 µL containing 3 µL of diluted genomic DNA, 1 µL (0.2 ng / µl) of each primer, 25 µL of master mix solution (Taq PCR Mastermix, Qiagen) and 20 µL of autoclaved Milli-Q water. Partial 18S, 28S sequences and the complete ITS region of the chytrid parasite were obtained with the following primers: EaF3 (Pröschold *et al.*, 2001), MH2 (Vandenkoornhuyse and Leyval, 1998), NS1, NS4, ITS4 (White *et al.*, 1990) and D3Ca (Lenaers *et al.*, 1989). The PCR parameters for each primer couple are specified in Table 1.

Note that the decreasing annealing temperature gradient for the primer couple MH2-NS4 aimed at increasing the specificity of the reaction in the first steps whilst favouring the DNA yield towards the end of the cycle. PCR products were separated by agar gel electrophoresis (35 min at 100 V on 1.5% agarose in TBE buffer) and multiple bands isolated by band excision with GeneJET Gel Extraction (Thermo Scientific) and purified by DNA clean-up Micro Kit (Thermo Scientific), followed by Sanger sequencing (GATC Biotech, Konstanz, Germany). Partial rDNA operon sequences were identified for two single cell isolates, SkChyt5 and SkChyt3. The longest sequence was obtained for isolate SkChyt5, for which 1464 bp within the 18S were obtained by merging the products of primers EaF3, NS1, MH2 (forward) and NS4 (reverse). The products of the reverse primers ITS4 (757 bp in the ITS region) and D3Ca (573 bp in the 28S), despite a good per base quality, were too short to be assembled with the rest of the rDNA operon. The partial 18S of a second single cell isolate, i.e. SkChyt3, was amplified via PCR using the primer couple MH2-NS4 and sequenced following the above described procedure, resulting in a 933 bp marker gene matching with 100% identity SkChyt5 18S. Therefore a 20 µL aliquot of the original MDA product from isolate SkChyt5 was diluted 1:4 (V:V) in autoclaved Milli-Q water and sent for genome library construction (NEBNext Ultra DNA

129 Library Prep Kit) and sequenced via Illumina Hiseq 3000 150 bp paired end sequencing (University of
130 Leeds Sequencing Facility, Leeds, United Kingdom).

131 2.4 *Genome querying for genetic barcodes*

132 FastQC (Andrews, 2010) was used to assess the quality of SkChyt5 Hiseq data (200,984,460 paired
133 end reads) before trimming with Trimmomatic (Bolger *et al.*, 2014, parameters detailed in
134 Supplementary Materials 1). The resulting SkChyt5 196,165,072 trimmed reads were queried via
135 BLAST (Altschul *et al.*, 1990) using in-house scripts (Supplementary Materials 1) designed to extract
136 subsets of reads as per their identity to a given query sequence. The best BLAST hit of SkChyt5 18S
137 amongst type material (i.e. *Kappamyces laurelensis* AFTOL-ID 690) was used to generate a
138 concatenated rDNA query sequence (GenBank accession numbers: DQ536478, DQ536494 and
139 DQ273824) to extract chytrid rDNA reads from the single cell genomic reads pool. The obtained
140 subset of reads (1453 merged reads) was *de novo* assembled into 13 contigs using Geneious 6.1.8
141 (Kearse *et al.*, 2012), of which 6 were retained on the basis of BLAST annotation (i.e. fungal rDNA)
142 and coverage (i.e. >10 reads; with 5 contigs out of 6 having a coverage >100 reads). The 6 selected
143 contigs were further merged to the SANGER sequences into two supercontigs, spanning the nearly
144 complete rDNA, but not overlapping.

145 In a complementary attempt to retrieve the complete rDNA operon, we generated a *de novo*
146 assembly of SkChyt5 in CLC Genomics Work Bench 8.5.1 (https://www.qiagenbioinformatics.com/)
147 and queried the resulting 299,415 contigs using the 18S sequence obtained by PCR on SkChyt5. This
148 approach resulted in the selection of 2 *de novo* assembled contigs of 1289 bp and 7688 bp in length,
149 both annotated as chytrids rDNA as per their best BLAST hit amongst cultured strains, i.e.
150 *Kappamyces laurelensis* isolate AFTOL-ID 690 18S (DQ536478.1) and *Boothiomyces macroporosum*
151 CBS 122107 28S (NG_027566.1) respectively. These two contigs were, when overlapping, 100 %
152 identical to all the sequences previously obtained by PCR and *in silico*. The 18S sequence obtained by
153 PCR filled the gap between the two contigs, allowing for the assembly of the complete rDNA operon,

which was retained for following phylogenetic analysis. The different methods used to reconstruct the full rDNA operon are summarized in Supplementary Figure 1. The rDNA operon was manually annotated in Geneious 6.1.8, by BLAST against Genebank. Introns were analysed with the same software in order to test whether they contained coding DNA sequences (CDS) and further annotated via UniProt. The entirety of the rDNA operon for the isolate SkChyt5 was deposited in GenBank under the accession number MH643793.

2.5 Phylogenetic reconstructions

A custom dataset of the 18S, 5.8S and 28S rDNA sequences of chytrids was built paying particular attention to sample diversity within the Rhizophydiales (Letcher *et al.*, 2006), since preliminary analysis pointed towards an inclusion of isolate SkChyt5 into this order. Sequences for each gene were aligned separately using the MAFFT (Katoh *et al.*, 2002) algorithm implemented in Geneious 6.1.8 and manually curated to remove the non-informative introns ITS1 and ITS2~~.~~. Substitution models were assessed for each gene separately in IQ-TREE 1.5.5 (Nguyen *et al.*, 2015) through ModelFinder (Kalyaanamoorthy *et al.*, 2017), resulting in TIM2+R5 (18S and 28S) and TPM2u+R4 (5.8S). A manual concatenation of the three alignments was then analysed in IQ-TREE 1.5.5 with a partitioned model (Chernomor *et al.*, 2016), allowing each gene to evolve at its own pace (–spp option). Phylogenetic reconstructions were computed with a Maximum Likelihood method using a 1000 replicates Ultrafast bootstrap approximation (UFBoot) test of phylogeny (Minh *et al.*, 2013). Aiming at including a better representation of uncultured environmental diversity, a phylogenetic reconstruction based on Rhizophydiales 18S was computed with the same above described procedure under the GTR+R4 model of molecular evolution. Finally, for consistency with previous work on Alphamycetaceae and Rhizophydiales phylogeny reconstructions (Letcher *et al.*, 2012; Seto and Degawa, 2018) we used a concatenation of 5.8S (substitution model SYM+I+G4) and 28S (substitution model TIM3+G4) to further confirm the phylogenetic position of our isolate.

2.6 Assessment of global distribution

The V4 hypervariable region of the 18S rDNA of isolate SkChy5 was used to query the raw metabarcode datasets of the Ocean Sampling Day through the Sequence Read Archive (SRA)(PRJEB8682, Kopf *et al.*, 2015) using an in-house script referred to as MOULINETTE which implements EDirect and SRA Toolkit utilities (Badis et al., *subm*.). Briefly, MOULINETTE extracts from SRA deposited metabarcoding datasets all reads matching a given query sequence above given identity, coverage and e-value thresholds. Here a rather stringent approach was used, i.e. reads were only retained when at least 99% identical over 80% of their length to the query sequence (refer to Suppl. Material 1 for details on the parameters used). Paired reads were filtered (expected error over 1.0) and aligned to the V4 hypervariable region of the 18S of isolate SkChyt5 in Geneious 6.1.8, resulting in two clusters divided by a shared synapomorphy (OTU1 and OTU2). Identity matrices were generated to investigate the percentage of identity between the reads and SkChyt5-V4-18S-rDNA with the same software. Sampling stations were deemed positive for the presence of the investigated organism, and therefore retained, when >10 merged paired reads were detected. For these stations GPS coordinates were extracted and maps generated using the open source online platform GPSVisualizer (http://www.gpsvisualizer.com/, Adam Schneider).

3. Results

3.1 Morphology

Infected *Skeletonema* cells were distinguished from healthy ones (Fig. 1A) thanks to the presence of nearly spherical sporangia growing epiphytically on diatom colonies (Fig. 1B). Infected cells showed signs of plasmolysis, chloroplast collapse (Fig. 1B) and decreased (if any) chlorophyll fluorescence ~~in UV light~~ (Fig. 1C). The majority of the observed sporangia had a diameter of ~ 5 µm, but reached 7.5 µm across in fully mature specimens. Sporangia were usually attached to the girdle band region of the infected cell. In a few instances however, sporangia could also be observed growing on the valvar surface within the cage of intercalary fultoportula processes connecting two adjacent *Skeletonema* cells (Fig. 1B, inlet). Examination of CW-stained sporangia ~~under UV light~~in epifluorescence highlighted the presence of a cell wall with distinct zones of wall thickening in

mature sporangia (Fig. 1C arrowheads). A reduced, unbranched rhizoidal system (Fig. 1C arrow) developed from the germ tube observed in encysted zoospores (Fig. 1C, arrow in the inlet). The presence of chitin was detected in sporangia cell walls, as shown by the positive reaction to the N-acetylglucosamine specific stain WGA-FITC (Fig. 1D~~,~~). Sporangia contain refractive lipid globules variable in size and number (Fig. 1E), whilst encysted zoospores contain a single lipid droplet (Fig. 1C, arrowhead,). Zoospores were sub-spherical, ~ 2.5 µm across, bearing a single whiplash flagellum (Fig. 1F-G, arrows) and a single refractive lipid droplet (Fig. 1F, arrowhead). Zoospores release or zoospore locomotion could never be directly observed. In one occasion a putative resting spore, with a thick cell wall and bearing a single eccentric refractive globule was observed (Fig. 1H). CW/NR staining highlighted the presence of a zoospore encysted on this structure, possibly suggestive of sexual reproduction (Fig. 1I).

3.3 Phylogenetic placement of isolate SkChyt5

Our maximum likelihood phylogenetic reconstruction on the concatenated rRNA encoding genes 18S, 5.8S and 28S (Fig. 2), retrieves the class Chytridiomycetes (*sensu* Powell & Letcher, 2014) and all the major chytrid orders, most of them with a high (> 98% UFboot) support. The core order Rhizophydiales is retrieved with 100% support to the exclusion of the genera *Batrachochytrium*, *Entophlyctis* and *Homoloaphlyctis*. The isolate SkChyt5 appears to cluster in a highly supported clade containing the family Kappamycetaceae and Alphamycetaceae; it falls within the latter family although with very weak support (43% UFboot). In a second reconstruction, consistently with previous Rhizophydiales phylogenies (Letcher *et al.*, 2012; Seto and Degawa, 2018), we assessed the phylogeny of the order Rhizophydiales using a concatenation of 5.8S and 28S (Fig. 3). Even if the clade composed by Kappamycetaceae and Alphamycetaceae was still retrieved with high support (99.2% UFboot), the overall result slightly changed, by including isolate SkChyt5 as a sister clade to *Gammamyces ourimbahiensis* and *Alphamyces chaetifer*, with moderate support (91% UFboot). Furthermore the family Alphamycetaceae appeared to be paraphyletic, with the genus *Betamyces* (93.5% UFboot) clustering as sister clade to the Kappamycetaceae. Finally, in order to be able to

assess the relationships between our isolate and the environmental diversity of Rhizophydiales, we computed an 18S-based phylogeny including environmental molecular data (Fig. 4). In this phylogenetic reconstruction, isolate SkChyt5 was found to be sister (96% UFboot) to *Betamyces* sp. isolate Barr-316 and three environmental sequences. The clade composed of Alphamycetaceae and Kappamycetaceae was once more strongly supported (100% UFboot) and encompassed a rich environmental diversity from lakes and high elevation soils from around the world. Within the 18S of SkChyt5 we identified two intronic sequences, one of which contained a CDS encoding a His-Cys box homing endonuclease as per its UniProt annotation (Q8TGE3).

3.4 Global distribution

Screening of the Ocean Sampling Day (Kopf *et al.*, 2015) metabarcoding dataset revealed the presence of organisms closely related to isolate SkChyt5 in 6 sampling stations across the North Atlantic (Fig. 5). The OSD project is a collaborative and global sequencing campaign aiming at analysing the marine microbial community annually on the summer solstice (21st of June). Here we screened the databased generated by the OSD 2014 campaign (PRJEB8682), during which seawater samples collected from 191 sites within exclusive economic zones (EEZs) around the world (see annexed map Suppl. Fig. 3) were filtered and processed for bulk DNA extraction and amplification of the 18S V4-hypervariable region with universal primers. Paired reads were from 96.5% to 100% identical to SkChyt5-V4-18S-rDNA and clustered in two different OTUs. Reads below an identity threshold of 98.4 % to SkChyt5-V4-18S-rDNA clustered in OTU2 (blue in Fig. 5) and shared a synapomorphy, which was not detected in any of the reads belonging to OUT1 (> 98.4 %, red in Fig. 5) nor in SkChyt5 18S sequence (Suppl. Figure 2). OTU1 was detected on both sides of the North Atlantic, in particular in Raunefjorden (Norway, 60°09'40.4"N, 5°06'54.1"E) and Booth Bay (Maine, USA, 43°50'39.8"N, 69°38'27.2"W), the former with a higher number of retrieved reads (n=67) as compared to the latter (n=34). Reads belonging to OTU2 were retrieved from the European Atlantic coasts only, with the highest read abundance (n=67) offshore Pasaia (Basque Country, Spain, 43°20'00.0"N, 1°55'30.0"W). Weaker read abundances associated to OTU2 have been detected in

two sampling stations offshore Belgium (n=27 in 51°16'10.3"N, 2°54'16.9"E and n=12 in 51°26'27.7"N, 3°08'23.8"E) and as far north as the Orkney Islands (n=21, 60°08'36.0"N 1°16'57.0"W).

Discussion

The overall thallus morphology of the parasitic organism infecting *Skeletonema* during the 2016 spring bloom already suggested its inclusion within the Chytridiomycota. Zoospores with a single whiplash flagellum and a lipid globule (Fig.1 C inlet, F, G), later developing in an endogenously generated monocentric thallus (Fig. 1 B inlet), are in line with extant descriptions of chytrid zoospores and with the definition of the *Chytridium*-type development given by Sparrow (1960). WGA-FITC highlighted the presence of chitin in the sporangia cell wall (Fig 1, D), a characteristic of true fungi useful in distinguishing chytrids from other unicellular parasites (Sparrow, 1960). As already observed in previous studies (Rasconi *et al.*, 2009), a better labelling of the rather inconspicuous intracellular rhizoidal system was obtained with the less selective stain Calcofluor White (Fig. 1 C arrow). Such a reduced rhizoidal system has already been reported for other parasitic Rhizophydiales interacting with their algal host via a “peg-like” rhizoid (Van den Wyngaert *et al.*, 2017). Calcofluor White staining also highlighted the presence of cell wall thickenings on the surface of mature sporangia (Fig. 1 C), reminiscent of the papillae, later developing into discharge pores, reported for many Rhizophydiales (Longcore, 2004; Letcher *et al.*, 2015) and other chytrid orders (Simmons *et al.*, 2009; Davis *et al.*, 2016). Unfortunately, spore discharge could not be directly observed in our samples; therefore the fate of the sporangia wall thickenings remains hypothetical. The rarely observed thick-walled structures, bearing a single eccentric lipid globule, clearly remind typical chytridiaceous resting spores (Longcore, 2004; Letcher and Powell, 2005; Letcher *et al.*, 2006). In Fig. 1 (H-I) epifluorescence microscopy and CW staining highlighted the presence of an encysted spore on one of these structures, consistent with one of the modality of sexual reproduction in the order Rhizophydiales, where a contributing spore (male gamete) encysts on a receptive thallus (female gamete), to which it transfers its cytoplasmic contents resulting in the

formation of the thick-walled resting spore (Sparrow, 1960; Van den Wyngaert *et al.*, 2017). In line with morphological evidence, the nearly complete rDNA operon obtained *in silico* for isolate SkChyt5 confirmed that this epibiotic parasite of *Skeletonema* belongs to the order Rhizophydiales in the phylum Chytridiomycota. Within this order, our isolate is firmly placed within a well-supported group composed of the families Alphamycetaceae and Kappamycetaceae (Letcher and Powell, 2005; Letcher *et al.*, 2012). However the *Skeletonema*-infecting chytrid does not clearly belong to any of these two families in our concatenated phylogenetic reconstruction (Fig. 2); instead, isolate SkChyt5 clusters sister to the Alphamycetaceae with a very weak ultrafast bootstrap support (43%). The family Alphamycetaceae is divided in two main groups; the first composed of the genus *Betamyces* alone and the second composed of the genera *Alphamyces* and *Gammamyces*. Those two main sub-clades have previously been found not to be supported by strong bootstraps (Letcher *et al.*, 2012; Seto and Degawa, 2018), a feature consistent with our 5.8S-28S phylogenetic reconstruction where the Alphamycetaceae appear paraphyletic (Fig. 3). Even if in this latter phylogenetic reconstruction the parasitoid of *Skeletonema* clusters closer to the genera *Alphamyces* and *Gammamyces,* any conclusion on the affinity of SkChyt5 to extant taxa would be assumptive. In the absence of taxonomically informative ~~information~~ data on zoospore ultrastructure (James *et al.*, 2000), and of a broader sequenced diversity within the Rhizophydiales as comparison, we refrain from any taxonomic treatment of the investigated *Skeletonema* parasitoid and we adopt the provisional name SkChyt, following published guidelines for temporary nomenclature for protists (Berney *et al.*, 2017).

We used phylogenetic analyses of molecular data from 18S-based metabarcoding surveys to assess whether chytrids related to SkChyt shared similar habitats or ecological strategies. High bootstrap support (96%, Fig. 4) places SkChyt5 sister to the saprobe *Betamyces sp.* Barr-316 (Smith *et al.*, 2014) and to a well-supported clade of isolates from freshwater Antarctic cyanobacterial mats (Jungblut *et al.*, 2012), a glacier forefield in Tibet (Khan and Kong, *unpublished*) and Japanese lakes (Ishida *et al.*, 2015). No marine isolate clusters close to SkChyt5 and only three isolates come from marine/brackish water in our phylogenetic reconstruction. This result is likely an artefact due to the

309 undersampling of the marine environment, potentially coupled with the marked seasonality shown
310 by chytrids in the plankton (Picard, 2017); the latter can be exacerbated in the case of parasites,
311 whose ephemeral presence and short lasting dynamics remain often undetected by molecular
312 surveys (Garvetto *et al.*, 2018). The global distribution of the SkChyt highlighted its presence in
313 coastal areas around the north Atlantic (Fig. 5). Since the Ocean Sampling Day 2014 campaign is
314 limited to coastal areas sampled at one time point (21st of June~~,~~ ~~(~~Kopf *et al.*, 2015), we cannot
315 exclude that SkChyt may also occur in the open sea. Likewise, we cannot rule out the hypothesis that
316 a strong seasonality for the studied chytrid (possibly driven by its diatom host) might have prevented
317 its detection in the southern hemisphere, where *Skeletonema* is virtually absent during the Austral
318 winter. Indeed, microscopic evidence of a chytrid parasite infecting *Skeletonema* sp. in the Humboldt
319 Current System off central Chile was recently reported, but unfortunately no matching molecular
320 data were~~as~~ available (Gutiérrez *et al.*, 2016). This chytrid was hypothesised to infect both
321 *Skeletonema* sp. and *Thalassiosira* sp. during the austral spring and late summer, therefore driving
322 the phytoplankton succession by allowing for the development of blooms of the immune diatom
323 *Chaetoceros* sp. On the other hand, one operational taxonomic unit (OTU14) closely related to
324 *Betamyces americaemeridionalis* ARG063, and therefore to SkChyt, was detected for three years
325 (2008, 2009 and 2011) in co-occurrence with *Chaetoceros* sp. dominated blooms in the English
326 Channel (Taylor and Cunliffe, 2016). Although no direct observation of parasitism exists, these
327 results strongly suggest that *Chaetoceros* might be a host of OTU14. Our observations do not allow
328 speculations on the infection of hosts other than *Skeletonema*, since both *Thalassiosira* and
329 *Chaetoceros* were present only in very low abundances in our samples, and none was found to bear
330 sporangia. The peculiar detached sporangia described in Gutiérrez *et al.* (2016) were not observed in
331 the samples investigated here, where all chytrid thalli grew epiphytically on *Skeletonema* colonies.

332 Our screening of metabarcoding datasets highlighted the presence of two OTUs clustering around
333 SkChyt5 with an identity varying from 100 to 98.4% (OTU1) and from 98.4 to 96.5% (OTU2). Each of
334 them shared synapomorphies on the V4 hypervariable region of the 18S rDNA gene (detailed in

335 Supplementary Figure 2), suggesting that these two OTUs correspond to genuine, distinct taxa.
336 Whether or not the two OTUs retrieved in this study belong to different yet closely related species,
337 the possibility that other chytrid parasites infecting marine diatoms fall within the clade
338 Alphamycetaceae/Kappamycetaceae should also be considered.

339 Thanks to the combination of PCR and Hiseq sequencing, we identified an intronic sequence one
340 base pair upstream the primer binding site used for the amplification of the V4 hypervariable region;
341 a second intron contains a coding sequence for a homing endonuclease enzyme, indicating that it is
342 active and spreading within SkChyt population (Chevalier and Stoddard, 2001). The presence of
343 intronic sequences, a well-known feature for the 18S ribosomal RNA of chytrids and other fungi
344 (Karpov *et al.*, 2017), may therefore interfere with the amplification of metabarcodes. It should be
345 envisaged that metabarcoding studies, despite their proven power in unveiling hidden planktonic
346 microbial diversity (de Vargas *et al.*, 2015), may suffer from such biases, especially towards certain
347 taxa. We argue that the caveats described here might have been causing a strong underappreciation
348 of the role of fungal parasites in controlling and affecting *Skeletonema* and other diatoms in the
349 global ocean, possibly causing biases in modelling biogeochemical cycling. To date, predation is
350 believed to be the largest source of mortality of phytoplankton (Calbet and Landry, 2004) causing
351 changes in prey physiology and behaviour (Amato *et al.*, 2018) with effects potentially cascading
352 throughout the food web; but little, if any, information on parasitism is included in marine food web
353 models. Examples from freshwater systems have been pointing towards the involvement of chytrids
354 in driving the succession of dominant phytoplankters (Van Donk and Ringelberg, 1983) and results
355 from (Gutiérrez *et al.*, 2016) seem to confirm these observations in the marine habitat. Molecular
356 markers obtained by SC analyses may constitute a useful tool to target taxa that remain undetected
357 in metabarcoding surveys, with the added benefit of potentially linking barcodes to ecological
358 functions, thus empowering the ecological interpretation of long term plankton time series. We
359 hope that he molecular data provided here will help triggering further investigation on the presence

and function of marine chytrids, which have the potential to be important drivers of phytoplankton dynamics and associated biogeochemical cycles in the ocean.

Acknowledgements

This project has received funding from the European Union's Horizon 2020 research and innovation programme under the Marie Skłodowska-Curie grant agreement No. 642575 (ALFF), the FP7 Marie Curie Actions PEOPLE-2007-2-2. ERG No. 230865, the grant agreement No. 727892 (GENIALG) and from the United Kingdom NERC under the grants GlobalSeaweed (NE/L013223/1) and MultiMARCAPP (NE/L013029/1).

Figure Captions

Table 1 Details of the parameters used for the PCR reactions carried out in this study.

Fig. 1 Microscopy observations of the chytrid parasite of *Skeletonema*. (A)Uninfected *Skeletonema* sp. chain; (B) Infected *Skeletonema* chain showing two spherical sporangia filled with refractive globular structures. Inset: Spherical sporangium filled with refractive globules, growing on the valvar surface of the host frustule, among fultoportula processes. (C) Calcofluor White staining (in blue) of the chytrid sporangia shown in (B). Note the presence of an infection plug (arrow) and various cell wall thickenings (arrowheads). Red chlorophyll autofluorescence of diatom phaeoplasts highlights the suffering of the sporangia-bearing cells. Inset: Encysted zoospore showing a germination tube (arrow) and a small Nile Red-positive lipid globule (arrowhead). (D) WGA-FITC staining (in green) of a chytrid sporangium in DIC (left) and epifluorescence (right). (E) Epifluorescence picture of a Nile Red-stained sporangium, highlighting the lipidic nature of the refractive globules observed in the sporangium. (F-G) Zoospores settled on the valvar surface of *Skeletonema*, showing the refractive lipid globule (arrowhead) and flagellum (arrows). (H) Putative resting spore, with thick cell wall and eccentric lipid globule in DIC. The blue colouring observed in DIC stems from the Evans Blue

385 counterstaining of Calcofluor White. (I) Epifluorescence observation of an attached zoospore to the
386 putative resting spore shown in (H). Scale bars = 5 µm.

387

388 **Fig. 2** Maximum Likelihood reconstruction (1000 Ultra-Fast Bootstraps) of chytrid phylogeny based
389 on three concatenated rRNA encoding gene sequences (18S, 5.8S and 28S). Symbols near the species
390 name indicate the presence (*) or absence (-) of genes encoding 18S, 5.8S and 28S respectively in
391 the alignment. The chytrid parasitoid of *Skeletonema* sp. SkChyt5 is highlighted in bold.

392

393 **Fig. 3** Maximum Likelihood phylogenetic reconstruction (1000 Ultra-Fast Bootstraps) of the order
394 Rhizophydiales based on the concatenated rDNA genes 5.8S and 28S. The chytrid parasitoid of
395 *Skeletonema* sp. is in bold.

396

397 **Fig. 4** Maximum Likelihood phylogenetic reconstruction (1000 Ultra-Fast Bootstraps) of the order
398 Rhizophydiales based on the 18S rDNA, taking into account environmental sequences from
399 metabarcoding surveys. The coloured dots besides the entries highlight ecological annotations:
400 freshwater (light blue), soil (brown), high elevation soil/snow/ice (grey), marine (dark blue), brackish
401 water (light and dark blue). A red "**P**" indicates entries known to be parasites. A white dot with "**?**"
402 indicates lack of information. Sequences of known taxonomic affiliation are in bold. The chytrid
403 parasitoid of *Skeletonema* SkChyt5 is highlighted by a larger font.

404 **Fig. 5** Map showing the distribution of OTUs related to the parasitoid of *Skeletonema* SkChyt5, as
405 reconstructed from the Ocean Sampling Day database. OTU1 (red) comprises reads matching
406 SkChyt5 rDNA-18S-V4 with an identity above 98,4 %, whilst OTU2 (blue) comprises reads identical to
407 the reference from 98,4 to 96.5 %. The diameter size of the points on the map is proportional to the
408 number of reads retrieved in the related sampling station, expressed by the digits within the circle.

409 The red star indicates the isolation point of SkChyt5 and the other biological samples used in this

410 study.

411 **Bibliography**

412 Altschul, S.F., Gish, W., Miller, W., Myers, E.W., and Lipman, D.J. (1990) Basic local alignment search
413 tool. *J. Mol. Biol.* **215**: 403–410.

414 Amato, A., Sabatino, V., Nylund, G.M., Bergkvist, J., Basu, S., Andersson, M.X., et al. (2018) Grazer-
415 induced transcriptomic and metabolomic response of the chain-forming diatom *Skeletonema*
416 *marinoi*. *ISME J.* 1594–1604.

417 Andrews, S. (2010) FastQC A Quality Control tool for High Throughput Sequence Data.
418 *http://www.bioinformatics.babraham.ac.uk/projects/fastqc/*.

419 Bergkvist, J., Thor, P., Jakobsen, H., and Selander, E. (2012) Grazer-induced chain length plasticity
420 reduces grazing risk in a marine diatom. **57**: 318–324.

421 Berney, C., Ciuprina, A., Bender, S., Brodie, J., Edgcomb, V., Kim, E., et al. (2017) UniEuk: Time to
422 Speak a Common Language in Protistology! *J. Eukaryot. Microbiol.* **64**: 407–411.

423 Bolger, A.M., Lohse, M., and Usadel, B. (2014) Trimmomatic: A flexible trimmer for Illumina
424 sequence data. *Bioinformatics* **30**: 2114–2120.

425 Borkman, D.G. and Smayda, T. (2009) Multidecadal (1959 – 1997) changes in *Skeletonema*
426 abundance and seasonal bloom patterns in Narragansett Bay , Rhode Island , USA. *J. Sea Res.*
427 **61**: 84–94.

428 Brown, S.P., Olson, B.J.S.C., and Jumpponen, A. (2015) Fungi and Algae Co-Occur in Snow : An Issue
429 of Shared Habitat or Algal Facilitation of Heterotrophs ? *Artic, Antart. Alp. Res.* **47**: 729–729.

430 De Bruin, A., Ibelings, B.W., Kagami, M., Mooij, W.M., and Van Donk, E. (2008) Adaptation of the
431 fungal parasite *Zygorhizidium planktonicum* during 200 generations of growth on
432 homogeneous and heterogeneous populations of its host, the diatom *Asterionella formosa*. *J.*
433 *Eukaryot. Microbiol.* **55**: 69–74.

434 Calbet, A. and Landry, M.R. (2004) Phytoplankton growth,microzooplankton grazing, and carbon
435 cycling in marine systems. *Limnol. Oceanogr.* **49**: 51–57.

436 Le Calvez, T., Burgaud, G., Mahé, S., Barbier, G., and Vandenkoornhuyse, P. (2009) Fungal diversity in
437 deep-sea hydrothermal ecosystems. *Appl. Environ. Microbiol.* **75**: 6415–6421.

438 Canesi, K.L. and Rynearson, T.A. (2016) Temporal variation of *Skeletonema* community composition
439 from a long-term time series in Narragansett Bay identified using high-throughput DNA
440 sequencing. *Mar. Ecol. Prog. Ser.* **556**: 1–16.

441 Canter, H.M. and Lund, J.W.G. (1953) Studies on plankton parasites. *Trans. Br. Mycol. Soc.* **36**: 13–37.

442 Chernomor, O., Von Haeseler, A., and Minh, B.Q. (2016) Terrace Aware Data Structure for
443 Phylogenomic Inference from Supermatrices. *Syst. Biol.* **65**: 997–1008.

444 Chevalier, B.S. and Stoddard, B.L. (2001) Homing endonucleases : structural and functional insight
445 into the catalysts of intron / intein mobility. *Nucleic Acids Res.* **29**: 3757–3774.

446 Comeau, A.M., Vincent, W.F., Bernier, L., and Lovejoy, C. (2016) Novel chytrid lineages dominate
447 fungal sequences in diverse marine and freshwater habitats. *Sci. Rep.* **6**: 30120.

448 Davis, W.J., Letcher, P.M., and Powell, M.J. (2016) *Triparticalcar equi* is a new coprophilus species
449 within Spizellomycetales, Chytridiomycota. *Phytologia* **98**: 241–249.

Van Donk, E. and Ringelberg, J. (1983) The effect of fungal parasitism on the succession of diatoms in Lake Maarsseveen I (The Netherlands). *Freshw. Biol.* **13**: 241–251.

Freeman, K.R., Martin, A.P., Karki, D., Lynch, R.C., Mitter, M.S., Meyer, A.F., et al. (2009) Evidence that chytrids dominate fungal communities in high-elevation soils. *Proc. Natl. Acad. Sci.* **106**: 18315–18320.

Frenken, T., Alacid, E., Berger, S.A., Bourne, E.C., Letcher, P.M., Loyau, A., et al. (2017) Integrating chytrid fungal parasites into plankton ecology : research gaps and needs. *Environ. Microbiol.* **19**: 3802–3822.

Garvetto, A., Nézan, E., Badis, Y., Bilien, G., Arce, P., Bresnan, E., et al. (2018) Novel Widespread Marine Oomycetes Parasitising Diatoms , Including the Toxic Genus *Pseudo-nitzschia* : Genetic , Morphological , and Ecological Characterisation. *Front. Microbiol.* **9**: 1–19.

Gleason, F.H., Kagami, M., Lefevre, E., and Sime-ngando, T. (2008) The ecology of chytrids in aquatic ecosystems : roles in food web dynamics. *Fungal Biol. Rev.* **22**: 17–25.

Grossart, H.P., Wurzbacher, C., James, T.Y., and Kagami, M. (2016) Discovery of dark matter fungi in aquatic ecosystems demands a reappraisal of the phylogeny and ecology of zoosporic fungi. *Fungal Ecol.* **19**: 28–38.

Gsell, A.S., de Senerpont Domis, L.N., Verhoeven, K.J.F., van Donk, E., and Ibelings, B.W. (2013) Chytrid epidemics may increase genetic diversity of a diatom spring-bloom. *ISME J.* **7**: 2057–9.

Gutiérrez, M.H., Jara, A.M., and Pantoja, S. (2016) Fungal parasites infect marine diatoms in the upwelling ecosystem of the Humboldt Current System off central Chile. *Environ. Microbiol.* **00**: 1–24.

Hassett, B.T., Ducluzeau, A.L., Collins, R.E., and Gradinger, R. (2017) Spatial distribution of aquatic marine fungi across the western Arctic and sub-Arctic. **19**: 475–484.

Hassett, B.T. and Gradinger, R. (2016) Chytrids dominate arctic marine fungal communities. *Environ. Microbiol.* **18**: 2001–2009.

Hibbett, D.S., Binder, M., Bischoff, J.F., Blackwell, M., Cannon, P.F., Eriksson, O.E., et al. (2007) A higher-level phylogenetic classification of the Fungi. *Mycol. Res.* **111**: 509–547.

Ibelings, B.W., De Bruin, A., Kagami, M., Rijkeboer, M., Brehm, M., and Donk, E. Van (2004) Host parasite interactions between freshwater phytoplankton and chytrid fungi (Chytridiomycota). *J. Phycol.* **40**: 437–453.

Ishida, S., Nozaki, D., Grossart, H.P., and Kagami, M. (2015) Novel basal, fungal lineages from freshwater phytoplankton and lake samples. *Environ. Microbiol. Rep.* **7**: 435–441.

James, T.Y., Porter, D., Leander, C. a., Vilgalys, R., and Longcore, J.E. (2000) Molecular phylogenetics of the Chytridiomycota supports the utility of ultrastructural data in chytrid systematics. *Can. J. Bot.* **78**: 336–350.

Jobard, M., Rasconi, S., Solinhac, L., Cauchie, H.M., and Sime-Ngando, T. (2012) Molecular and morphological diversity of fungi and the associated functions in three European nearby lakes. *Environ. Microbiol.* **14**: 2480–2494.

Jungblut, A.D., Vincent, W.F., and Lovejoy, C. (2012) Eukaryotes in Arctic and Antarctic cyanobacterial mats. *FEMS Microbiol. Ecol.* **82**: 416–428.

Kagami, M., Miki, T., and Takimoto, G. (2014) Mycoloop: Chytrids in aquatic food webs. *Front. Microbiol.* **5**: 1–9.

Kalyaanamoorthy, S., Minh, B.Q., Wong, T.K.F., von Haeseler, A., and Jermiin, L.S. (2017) ModelFinder: fast model selection for accurate phylogenetic estimates. *Nat. Methods* **14**: 587–589.

Karpov, S.A., Mamanazarova, K.S., Popova, O. V, Aleoshin, V. V, James, T.Y., Mamkaeva, M.A., et al. (2017) Monoblepharidomycetes diversity includes new parasitic and saprotrophic species with highly intronized rDNA. *Fungal Biol.* **121**: 729–741.

Katoh, K., Misawa, K., Juma, K., and Miyata, T. (2002) MAFFT: a novel method for rapid multiple sequence alignment based on fast Fourier transform. *Nucleic Acids Res.* **30**: 3059–3066.

Kearse, M., Moir, R., Wilson, A., Stones-havas, S., Sturrock, S., Buxton, S., et al. (2012) Geneious Basic : An integrated and extendable desktop software platform for the organization and analysis of sequence data. *Bioinformatics* **28**: 1647–1649.

Kopf, A., Bicak, M., Kottmann, R., Schnetzer, J., Kostadinov, I., Lehmann, K., et al. (2015) The ocean sampling day consortium. *Gigascience* **4**: 27.

Lasken, R.S. (2007) Single-cell genomic sequencing using Multiple Displacement Amplification. *Curr. Opin. Microbiol.* **10**: 510–516.

Lenaers, G., Michot, L.M.B., and Herzog, M. (1989) Dinoflagellates in Evolution . A Molecular Phylogenetic Analysis of Large Subunit Ribosomal RNA. 40–51.

Lepère, C., Ostrowski, M., Hartmann, M., Zubkov, M. V, and Scanlan, D.J. (2016) In situ associations between marine photosynthetic picoeukaryotes and potential parasites – a role for fungi? *Environ. Microbiol. Rep.* **8**: 445–451.

Letcher, P.M. and Powell, M.J. (2005) *Kappamyces*, a new genus in the Chytridiales (Chytridiomycota). *Nov. Hedwigia* **80**: 115–133.

Letcher, P.M., Powell, M.J., Churchill, P.F., and Chambers, J.G. (2006) Ultrastructural and molecular phylogenetic delineation of a new order, the Rhizophydiales (Chytridiomycota). *Mycol. Res.* **110**: 898–915.

Letcher, P.M., Powell, M.J., and Davis, W.J. (2015) A new family and four new genera in Rhizophydiales (Chytridiomycota). *Mycologia* **107**: 808–830.

Letcher, P.M., Vélez, C.G., Schultz, S., and Powell, M.J. (2012) New taxa are delineated in Alphamycetaceae (Rhizophydiales, Chytridiomycota). *Nov. Hedwigia* **94**: 9–29.

Longcore, J.E. (2004) *Rhizophydium brooksianum* sp . nov ., a multipored chytrid from soil. *Mycologia* **96**: 162–171.

Minh, B.Q., Anh, M., Nguyen, T., and Haeseler, A. Von (2013) Ultrafast Approximation for Phylogenetic Bootstrap. *Mol. Biol. Evol.* **30**: 1188–1195.

Monchy, S., Sanciu, G., Jobard, M., Rasconi, S., Gerphagnon, M., Chabé, M., et al. (2011) Exploring and quantifying fungal diversity in freshwater lake ecosystems using rDNA cloning / sequencing and SSU tag pyrosequencing. *Environ. Microbiol.* **13**: 1433–1453.

Naff, C.S., Darcy, J.L., and Schmidt, S.K. (2013) Phylogeny and biogeography of an uncultured clade of snow chytrids. *Environ. Microbiol.* **15**: 2672–2680.

Nguyen, L.T., Schmidt, H.A., Von Haeseler, A., and Minh, B.Q. (2015) IQ-TREE: A fast and effective stochastic algorithm for estimating maximum-likelihood phylogenies. *Mol. Biol. Evol.* **32**: 268–274.

Picard, K.T. (2017) Coastal marine habitats harbor novel early-diverging fungal diversity. *Fungal Ecol.* **25**: 1–13.

Powell, M. J. & Letcher, P.M. (2014) Chytridiomycota, Monoblepharidomycota and Neocallimastigomycota. In, McLaughlin,D.J. and Spatafora,J.W. (eds), *The Mycota VII, Systematics and Evolution, Part A.* Springer-Verlag, Heidelberg, pp. 141–175.

Pröschold, T., Marin, B., Gert, U., and Melkonian, M. (2001) Molecular Phylogeny and Taxonomic Revision of *Chlamydomonas* (Chlorophyta). I . Emendation of *Chlamydomonas* Ehrenberg and *Chloromonas* Gobi , and Description of *Oogamochlamys* gen . nov . and *Lobochlamys* gen . nov . 1. *Protist* **152**: 265–300.

Rad-Menéndez, C., Gerphagnon, M., Garvetto, A., Arce, P., Badis, Y., and Gachon, C.M.M. (2018) Rediscovering *Zygorhizidium affluens* Canter - Molecular taxonomy, infectious cycle, and cryopreservation of a chytrid infecting the bloom-forming diatom *Asterionella formosa*. *Appl. Environ. Microbiol.* **84**:.

Rasconi, S., Jobard, M., Jouve, L., and Sime-Ngando, T. (2009) Use of calcofluor white for detection, identification, and quantification of phytoplanktonic fungal parasites. *Appl. Environ. Microbiol.* **75**: 2545–2553.

Seto, K. and Degawa, Y. (2018) *Collimyces mutans* gen . et sp . nov . (Rhizophydiales , Collimycetaceae fam . nov .), a New Chytrid Parasite of *Microglena* (Volvocales , clade Monadinia). *Protist* **169**: 507–520.

Simmons, D.R., James, T.Y., Meyer, A.F., and Longcore, J.E. (2009) Lobulomycetales, a new order in the Chytridiomycota. *Mycol. Res.* **113**: 450–460.

Smith, D.S., Rocheleau, H., Chapados, J.T., Abbott, C., Ribero, S., Redhead, S.A., et al. (2014) Phylogeny of the Genus *Synchytrium* and the Development of TaqMan PCR Assay for Sensitive Detection of *Synchytrium endobioticum* in Soil. *Phytopathology* **104**: 422–432.

Sparrow, F. (1960) Aquatic Phycomycetes The University of Michigan Press, Ann Arbor.

Sparrow, F.K. (1958) Interrelatioinships and phylogeny of the aquatic phycomyecetes. *Mycologia* **50**: 797–813.

Taylor, J.D. and Cunliffe, M. (2016) Multi-year assessment of coastal planktonic fungi reveals environmental drivers of diversity and abundance. *ISME J.* 1–11.

Vandenkoornhuyse, P. and Leyval, C. (1998) SSU rDNA Sequencing and PCR-Fingerprinting Reveal Genetic Variation within *Glomus mosseae*. *Mycologia* **90**: 791–797.

de Vargas, C., Audic, S., Henry, N., Decelle, J., Mahe, F., Logares, R., et al. (2015) Eukaryotic plankton diversity in the sunlit ocean. *Science (80-.).* **348**: 1–11.

White, T.J., Bruns, T., Lee, S., and Taylor, J. (1990) Amplification and direct sequencing of fungal ribosomal RNA genes for phyologenetics. In, Innis,M.A., Gelfand,D.H., Sninsky,J.J., and White,T.J. (eds), *PCR protocols: A Guide to Methods and Applications*. Academic Press, Inc., New York, pp. 315–322.

570 Van den Wyngaert, S., Seto, K., Rojas-Jimenez, K., Kagami, M., and Grossart, H.P. (2017) A New
571 Parasitic Chytrid, *Staurastromyces oculus* (Rhizophydiales, Staurastromycetaceae fam. nov.),
572 Infecting the Freshwater Desmid *Staurastrum* sp. *Protist* **168**: 392–407.

573

574

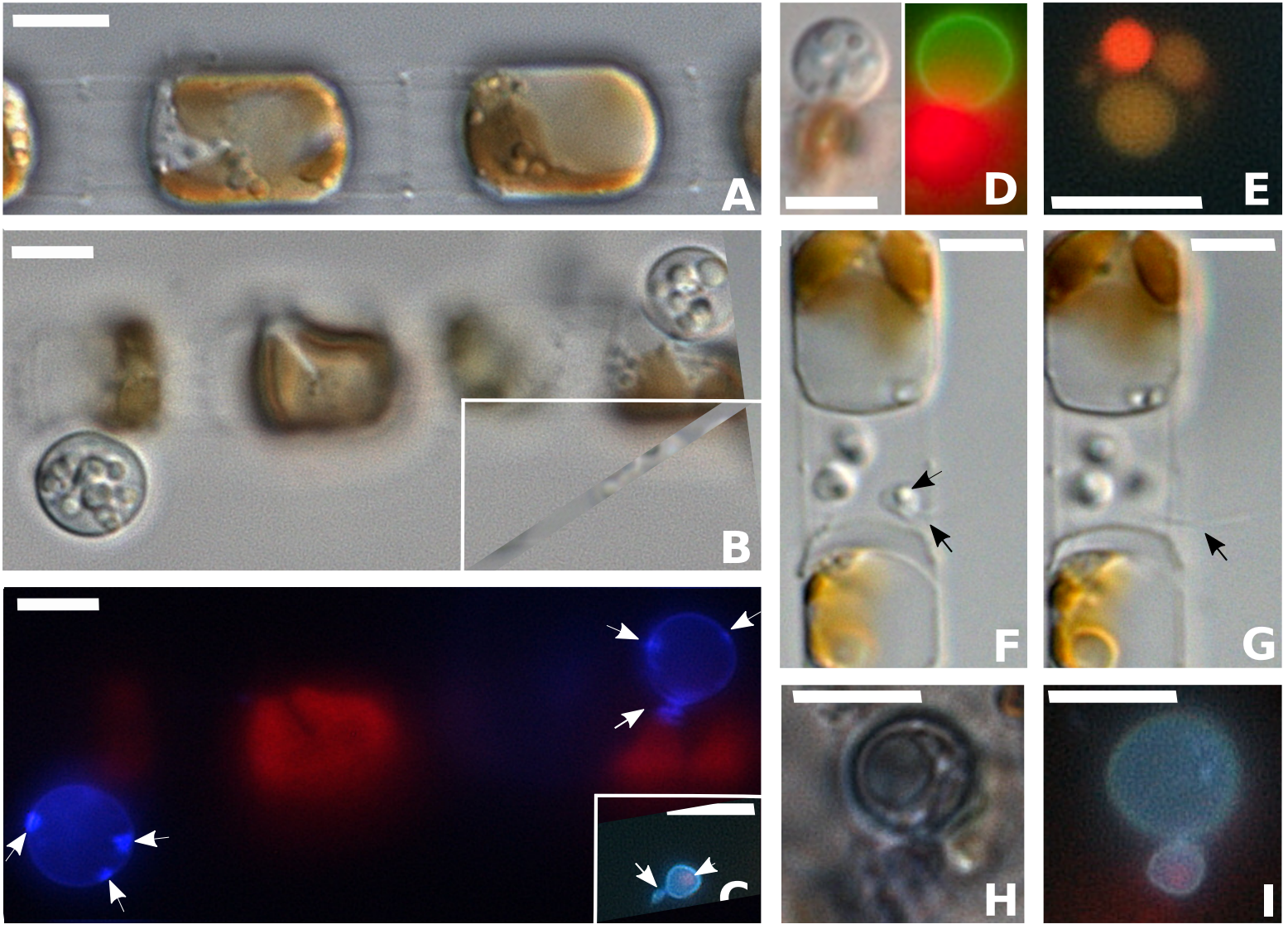
A
B
C
D
E
F
G
H
I

Boothiomyces macroporosum PL AUS21 ***
Terramyces subangulosum PL 122 -**
Boothiomyces sp. ARG040 -**
Terramycetaceae
Dinomyces arenysensis P237 --* Dinomycetaceae
Coralloidiomyces digitatus -** Coralloidiomycetaceae
Globomyces pollinis-pini ARG068 -**
Urceomyces sphaerocarpus ARG048 -**
Globomycetaceae
Uebelmesseromyces harderi JEL171 *** Ubelmesseromycetacea
Operculomyces laminatus JEL223 -** Operculomycetaceae
Pateramyces corrientinensis ARG046 -** Pateramycetaceae
Staurastromyces oculus STAU-CHY3 *** Staurastromycetaceae
Rhizophydium brooksianum JEL136 ***
Rhizophydium globosum JEL222 -**
Rhizophydium sp. ARG051 -**
Rhizophydium sp. ARG016 -**
Rhizophydiaceae
Protrudomyces lateralis ARG072 -** Protrudromycetaceae
Aquamyces chlorogonii *** Aquamycetaceae
Angulomyces argentinensis *** Angulomycetaceae
Paranamyces uniporus WJD158 -**
Halomyces littoreus ***
Paludomyces mangrovei ATCC26191 -**
Halomycetaceae
Kappamyces laurelensis isolate AFTOL-ID 690 ***
Kappamyces laurelensis PL 98 ***
Kappamycetaceae
Skeletonema parasitoid SkChyt5 *
Alphamyces chaetifer ***
Gammamyces ourimbahensis PL 116 -**
Betamyces sp. PL 173 -**
Betamyces sp. Barr-316 ***
Betamyces americameridionalis ARG063 -**
Alphamycetaceae
Collimyces mutans KS100 *** Collimycetaceae
Homoloaphlyctis polyrhiza JEL 142 ***
Entophlyctis helioformis AFTOL-ID-40 ***
Entophlyctis helioformis JEL122 ***
Batrachochytrium salamandrivorans AMFP13/1 ***
Batrachochytrium dendrobatidis JEL197 ***
uncultured Chytridiomycota PFH9SP2005 *--
uncultured Chytridiomycota AY2009D3 *--
uncultured Chytridiomycota PA2009E8 *--
uncultured Chytridiomycota PA2009B8 *--
Novel Clade II
sensu Lefèvre et al. 2008
Karlingiomyces asterocystis JEL 572 *-*
Arkaya lepida JEL 93 ***
Lacustromyces hiemalis JEL 31 *-*
Polychytrium aggregatum JEL 109 ***
Polychytriales
uncultured eukaryote 281A01*--
uncultured Chytridiomycota PA2009D11 **-
uncultured Chytridiomycota AY2009B15 **-
Zygorhizidium aff. melosirae KS99 ***
Zygorhizidium planktonicum KS98 ***
Novel Clade II
sensu Jobard et al. 2012
Rhizophlyctis rosea UCB57-5 *--
Rhizophlyctis rosea UCB47-07 *--
Rhizophlyctis rosea JEL 318 ***
Rhizophlyctidiales
Gaertneriomyces semiglobifer UCB91-10 ***
Thoreauomyces humboldtii JEL 95 ***
Spizellomyces punctatus ATCC48900 ***
Spizellomycetales sp. JEL 355 ***
Spizellomycetales
Cladochytrium replicatum JEL 180 ***
Nowakowskiella sp. JEL 127 ***
Cladochytriales sp. JEL 72 ***
Allochytridium luteum JEL 324 ***
Cladochytriales
Dendrochytridium crassum JEL 354 ***
Phlyctochytrium planicorne JEL 47 ***
Pseudorhizidium endosporangiatum JEL 221 ***
Rhizophydium planktonicum B5 *--
Chytriomyces hyalinus MP4 ***
Entophlyctis luteolus JEL 129 *-*
Rhizoclosmatium sp. JEL 347-h ***
Podochytrium dentatum JEL 30 ***
Obelidium mucronatum JEL 57 ***
Chytridiales
Gromochytrium mamkaevae CALU X-51 ***
uncultured eukaryote kor 110904 17 *--
Gromochytriales
Mesochytrium penetrans CALU X-10 *-*
uncultured Chytridiomycota PFF5SP2005 *--
uncultured Chytridiomycota T2P1AeB05 *--
Mesochytriales
Alogomyces tanneri ***
Chytridium polysiphoniae *--
Lobulomycetales sp. AF017 *-*
Clydaea vesicula isolate JEL 369 ***
Lobulomyces poculatus JEL 343 ***
Lobulomyces angularis JEL 45 ***
Lobulomycetales
Allomyces arbusculus Brazil2 ***
Blastocladiella emersonii UCB49-1 ***
Catenophlyctis sp. JEL 298 ***
Blastocladiomycota
Hyaloraphidium curvatum SAG235-1 **-
Oedogoniomyces sp. CR84 ***
Gonapodya sp. JEL 183 ***
Monoblepharella mexicana UCB78-1 ***
Monoblepharidiomycetes
Cyllamyces aberensis EO14 ***
Neocallimastix sp. GE13 ***
Orpinomyces sp. OUS1 ***
Neocallimastigomycota
Rozella allomycis UCB47-054 ***
Rozella sp. JEL 347 ***
Outgroup (Cryptomycota)
Rhizophydiales
Chytridiomycetes
0.1

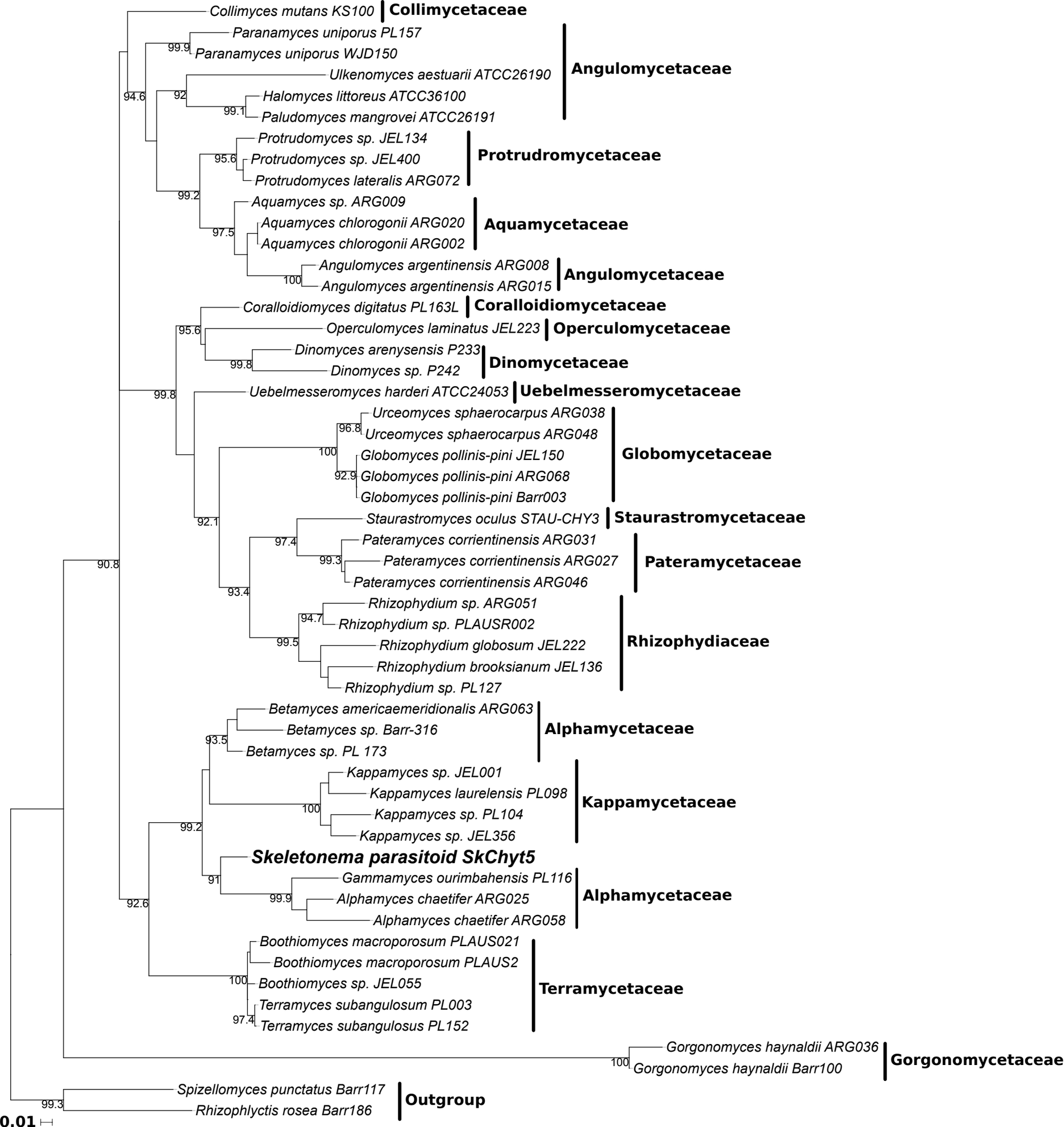
Collimyces mutans KS100
Collimycetaceae
Paranamyces uniporus PL157
Paranamyces uniporus WJD150
Ulkenomyces aestuarii ATCC26190
Halomyces littoreus ATCC36100
Paludomyces mangrovei ATCC26191
Angulomycetaceae
Protrudomyces sp. JEL134
Protrudomyces sp. JEL400
Protrudomyces lateralis ARG072
Protrudromycetaceae
Aquamyces sp. ARG009
Aquamyces chlorogonii ARG020
Aquamyces chlorogonii ARG002
Aquamycetaceae
Angulomyces argentinensis ARG008
Angulomyces argentinensis ARG015
Angulomycetaceae
Coralloidiomyces digitatus PL163L
Coralloidiomycetaceae
Operculomyces laminatus JEL223
Operculomycetaceae
Dinomyces arenysensis P233
Dinomyces sp. P242
Dinomycetaceae
Uebelmesseromyces harderi ATCC24053
Uebelmesseromycetaceae
Urceomyces sphaerocarpus ARG038
Urceomyces sphaerocarpus ARG048
Globomyces pollinis-pini JEL150
Globomyces pollinis-pini ARG068
Globomyces pollinis-pini Barr003
Globomycetaceae
Staurastromyces oculus STAU-CHY3
Staurastromycetaceae
Pateramyces corrientinensis ARG031
Pateramyces corrientinensis ARG027
Pateramyces corrientinensis ARG046
Pateramycetaceae
Rhizophydium sp. ARG051
Rhizophydium sp. PLAUSR002
Rhizophydium globosum JEL222
Rhizophydium brooksianum JEL136
Rhizophydium sp. PL127
Rhizophydiaceae
Betamyces americaemeridionalis ARG063
Betamyces sp. Barr-316
Betamyces sp. PL 173
Alphamycetaceae
Kappamyces sp. JEL001
Kappamyces laurelensis PL098
Kappamyces sp. PL104
Kappamyces sp. JEL356
Kappamycetaceae
Skeletonema parasitoid SkChyt5
Gammamyces ourimbahensis PL116
Alphamyces chaetifer ARG025
Alphamyces chaetifer ARG058
Alphamycetaceae
Boothiomyces macroporosum PLAUS021
Boothiomyces macroporosum PLAUS2
Boothiomyces sp. JEL055
Terramyces subangulosum PL003
Terramyces subangulosus PL152
Terramycetaceae
Gorgonomyces haynaldii ARG036
Gorgonomyces haynaldii Barr100
Gorgonomycetaceae
Spizellomyces punctatus Barr117
Rhizophlyctis rosea Barr186
Outgroup
94.6
99.9
92
99.1
95.6
99.2
97.5
100
95.6
99.8
99.8
96.8
100
92.9
92.1
97.4
99.3
90.8
93.4
94.7
99.5
93.5
100
99.2
91
99.9
92.6
100
97.4
99.3
0.01

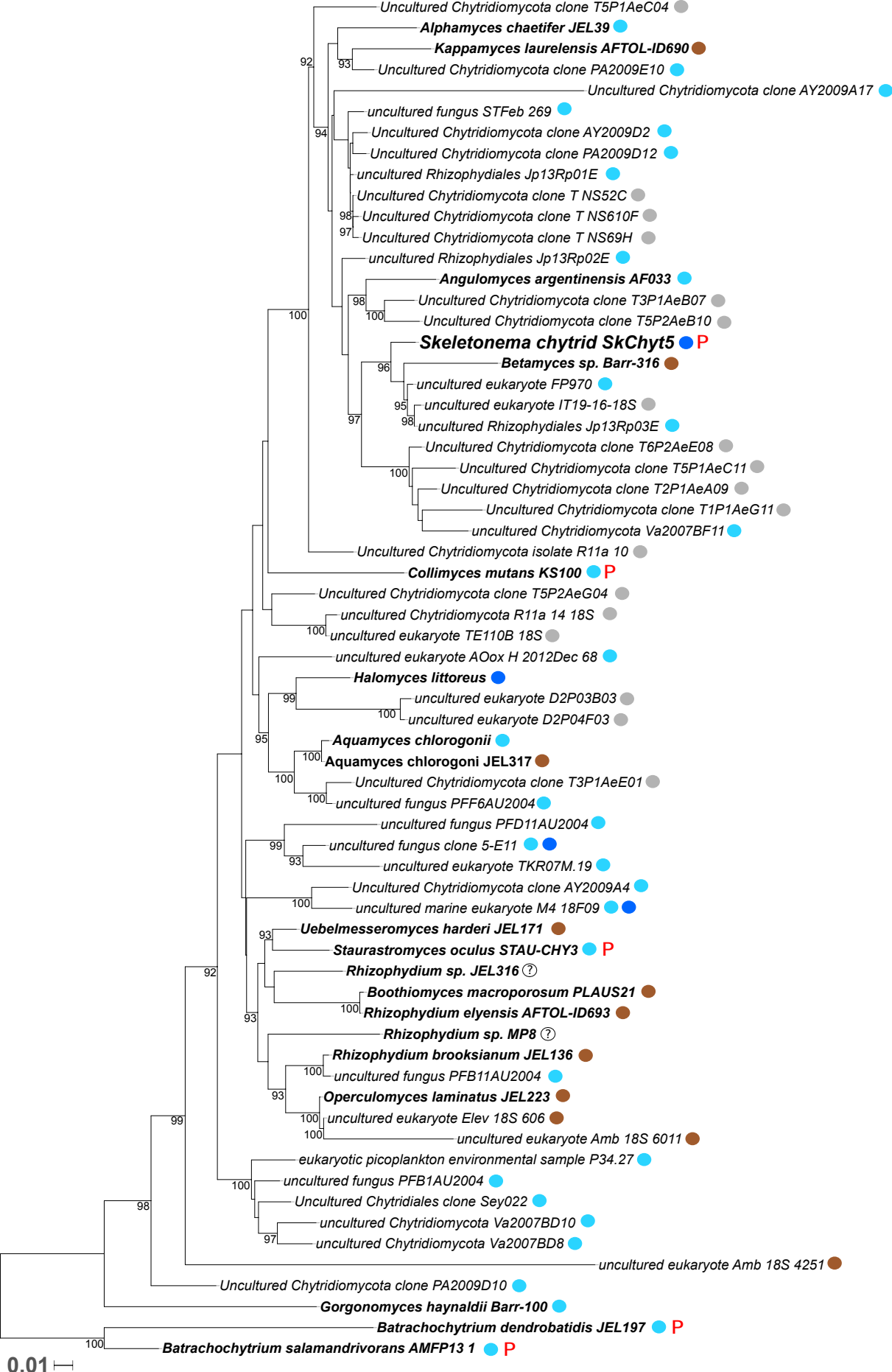
Uncultured Chytridiomycota clone T5P1AeC04
Alphamyces chaetifer JEL39
Kappamyces laurelensis AFTOL-ID690
Uncultured Chytridiomycota clone PA2009E10
Uncultured Chytridiomycota clone AY2009A17
uncultured fungus STFeb 269
Uncultured Chytridiomycota clone AY2009D2
Uncultured Chytridiomycota clone PA2009D12
uncultured Rhizophydiales Jp13Rp01E
Uncultured Chytridiomycota clone T NS52C
Uncultured Chytridiomycota clone T NS610F
Uncultured Chytridiomycota clone T NS69H
uncultured Rhizophydiales Jp13Rp02E
Angulomyces argentinensis AF033
Uncultured Chytridiomycota clone T3P1AeB07
Uncultured Chytridiomycota clone T5P2AeB10
Skeletonema chytrid SkChyt5 P
Betamyces sp. Barr-316
uncultured eukaryote FP970
uncultured eukaryote IT19-16-18S
uncultured Rhizophydiales Jp13Rp03E
Uncultured Chytridiomycota clone T6P2AeE08
Uncultured Chytridiomycota clone T5P1AeC11
Uncultured Chytridiomycota clone T2P1AeA09
Uncultured Chytridiomycota clone T1P1AeG11
uncultured Chytridiomycota Va2007BF11
Uncultured Chytridiomycota isolate R11a 10
Collimyces mutans KS100 P
Uncultured Chytridiomycota clone T5P2AeG04
uncultured Chytridiomycota R11a 14 18S
uncultured eukaryote TE110B 18S
uncultured eukaryote AOox H 2012Dec 68
Halomyces littoreus
uncultured eukaryote D2P03B03
uncultured eukaryote D2P04F03
Aquamyces chlorogonii
Aquamyces chlorogoni JEL317
Uncultured Chytridiomycota clone T3P1AeE01
uncultured fungus PFF6AU2004
uncultured fungus PFD11AU2004
uncultured fungus clone 5-E11
uncultured eukaryote TKR07M.19
Uncultured Chytridiomycota clone AY2009A4
uncultured marine eukaryote M4 18F09
Uebelmesseromyces harderi JEL171
Staurastromyces oculus STAU-CHY3 P
Rhizophydium sp. JEL316 ?
Boothiomyces macroporosum PLAUS21
Rhizophydium elyensis AFTOL-ID693
Rhizophydium sp. MP8 ?
Rhizophydium brooksianum JEL136
uncultured fungus PFB11AU2004
Operculomyces laminatus JEL223
uncultured eukaryote Elev 18S 606
uncultured eukaryote Amb 18S 6011
eukaryotic picoplankton environmental sample P34.27
uncultured fungus PFB1AU2004
Uncultured Chytridiales clone Sey022
uncultured Chytridiomycota Va2007BD10
uncultured Chytridiomycota Va2007BD8
uncultured eukaryote Amb 18S 4251
Uncultured Chytridiomycota clone PA2009D10
Gorgonomyces haynaldii Barr-100
Batrachochytrium dendrobatidis JEL197 P
Batrachochytrium salamandrivorans AMFP13 1 P
0.01

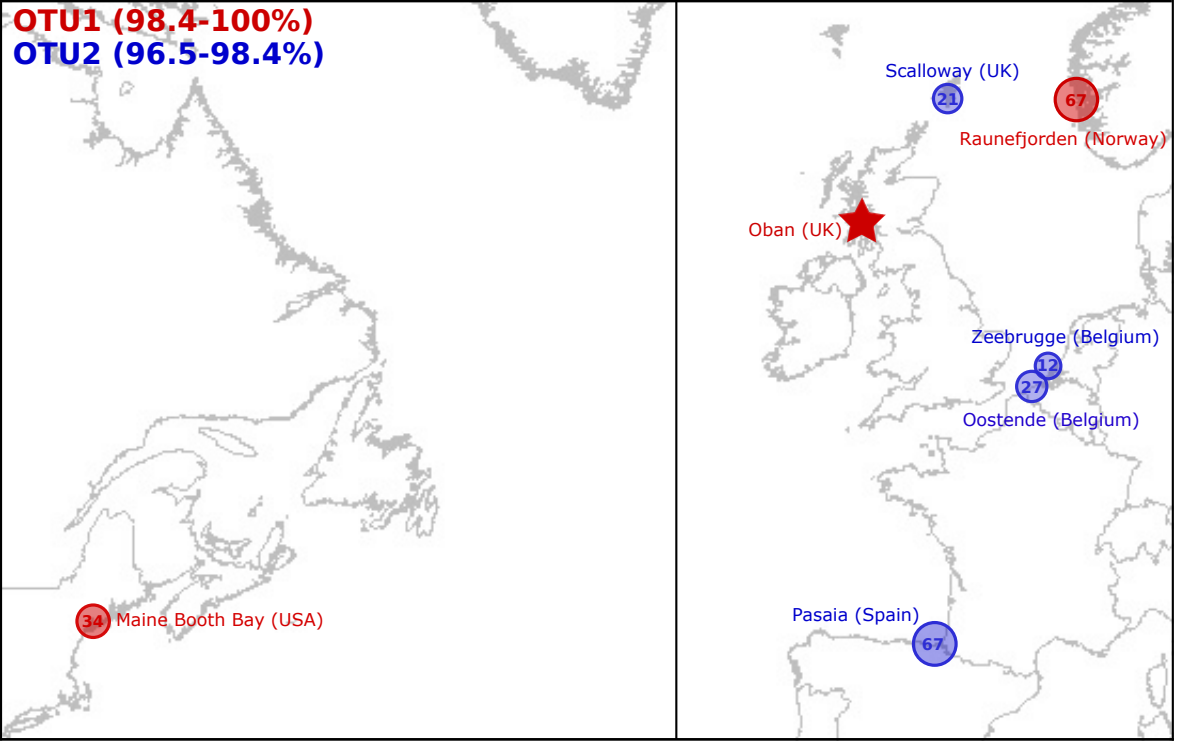
OTU1 (98.4-100%)
OTU2 (96.5-98.4%)
34
Maine Booth Bay (USA)
Scalloway (UK)
21
67
Raunefjorden (Norway)
Oban (UK)
Zeebrugge (Belgium)
12
27
Oostende (Belgium)
Pasaia (Spain)
67

Primer Couple	1st Step (Denaturation)	2nd Step (Amplification)				3rd Step (Elongation)
		Denaturation	Annealing	Elongation	Number of Cycles	
MH2-NS4	94˚C x 3 min	94˚C x 30 s	58˚C x 1 min	72˚Cx 1 min	5	72˚C x 5 min
		94˚C x 30 s	55˚C x 1 min	72˚Cx 1 min	10	
		94˚C x 30 s	52˚C x 1 min	72˚Cx 1 min	13	
		94˚C x 30 s	48˚C x 1 min	72˚Cx 1 min	17	
NS1-ITS4	94˚C x 30 s	94˚C x 15 s	48˚C x 1 min	65˚Cx 3 min	30	65˚C x 10 min
EaF3-D3Ca	94˚C x 30 s	94˚C x 15 s	58˚C x 1 min	65˚Cx 3 min	30	65˚C x 10 min

Supplementary Figure 1: PCR and *in silico* reconstruction of **SkChyt5** rDNA

Legend:

PCR : primers detailed in the figure on each PCR product.

Guided assembly approach: contigs retrieved by the customised pipeline (Supplementary material 1, ContigBlaster_V8.sh) using *Kappamyces laurelensis* AFTOL-ID 690 (DQ536478, DQ536494 and DQ273824) as query gene on the dataset of paired and reads. The resulting subset (1453 reads) was afterwards assembled in Geneious (KL_CONTIGs in figure below).

***De novo* approach:** contigs retrieved by the customised pipeline (Supplementary material 1, ContigBlaster_V8.sh) using SkChyt5 18S retrieved by PCR (MH2-NS4) as query gene on the contig dataset generated by unsupervised assembly of paired end reads in CLC Genomics Work Bench 8 (DeNovo_CONTIG in figure below).

PCR products and contigs retrieved by both methods match with 100% identity

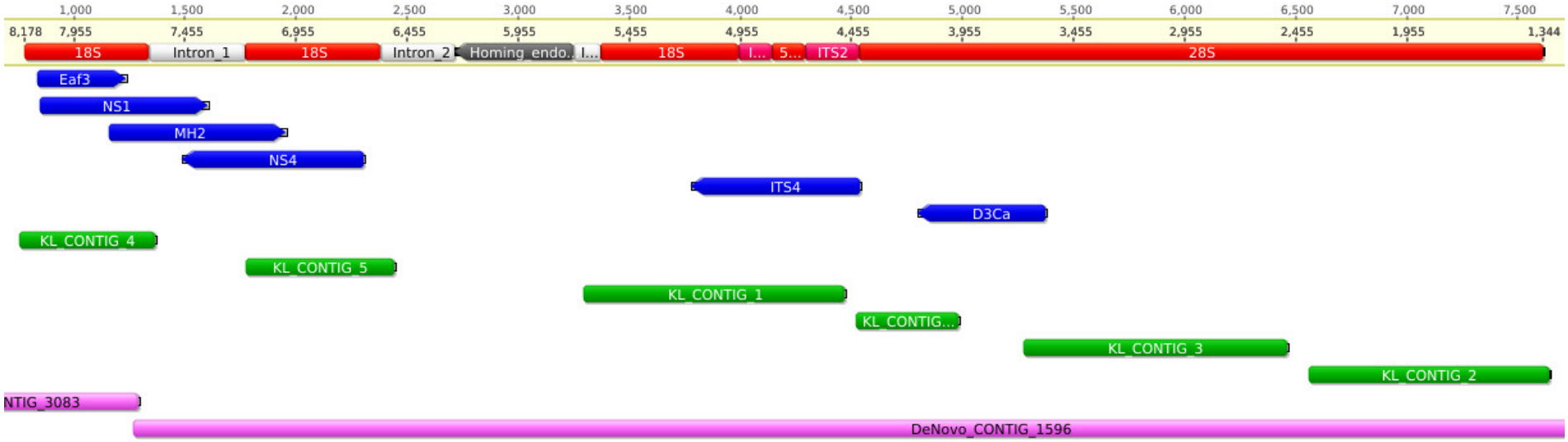

Supplementary Figure 2: Synapomorphies detected in OTU 1 and OTU 2

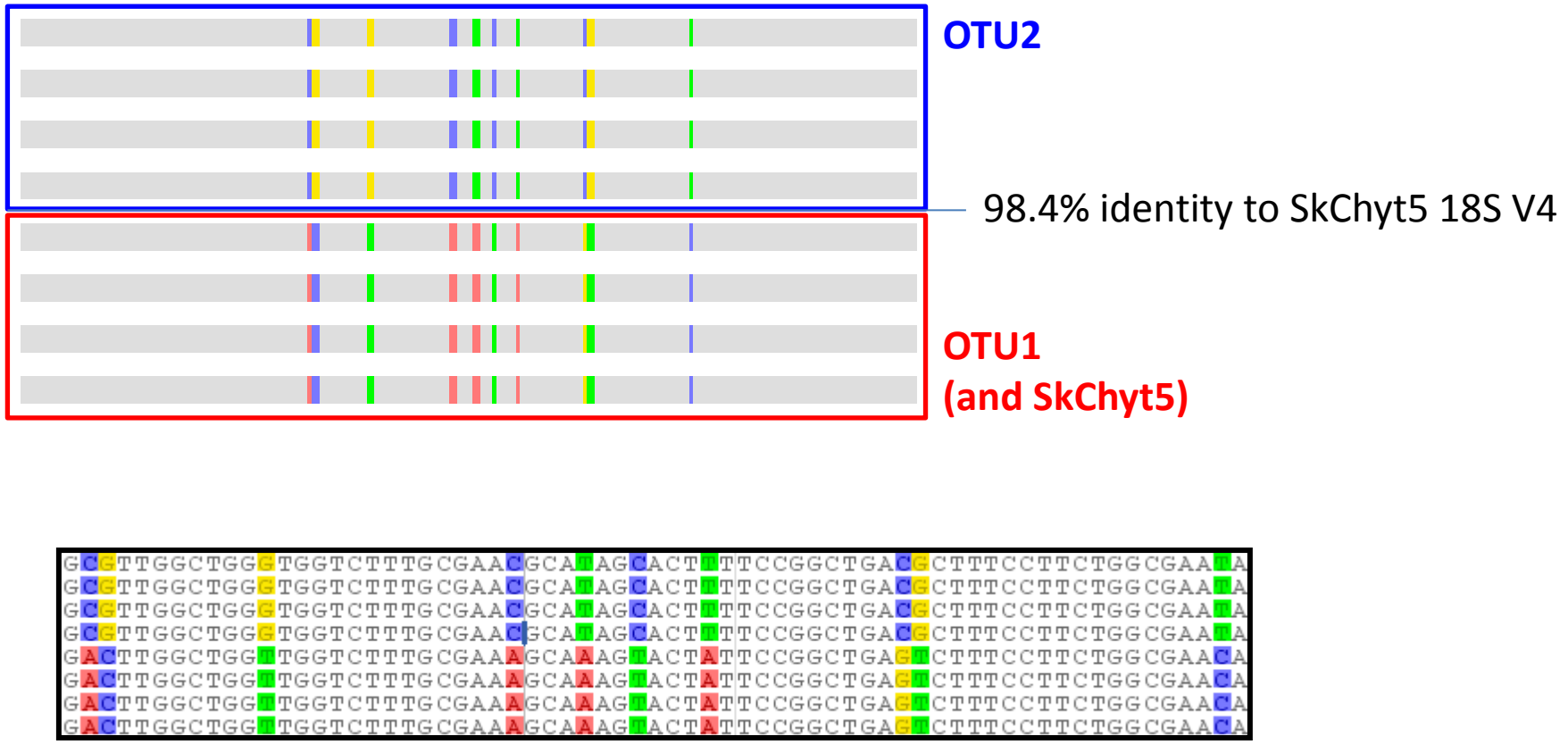

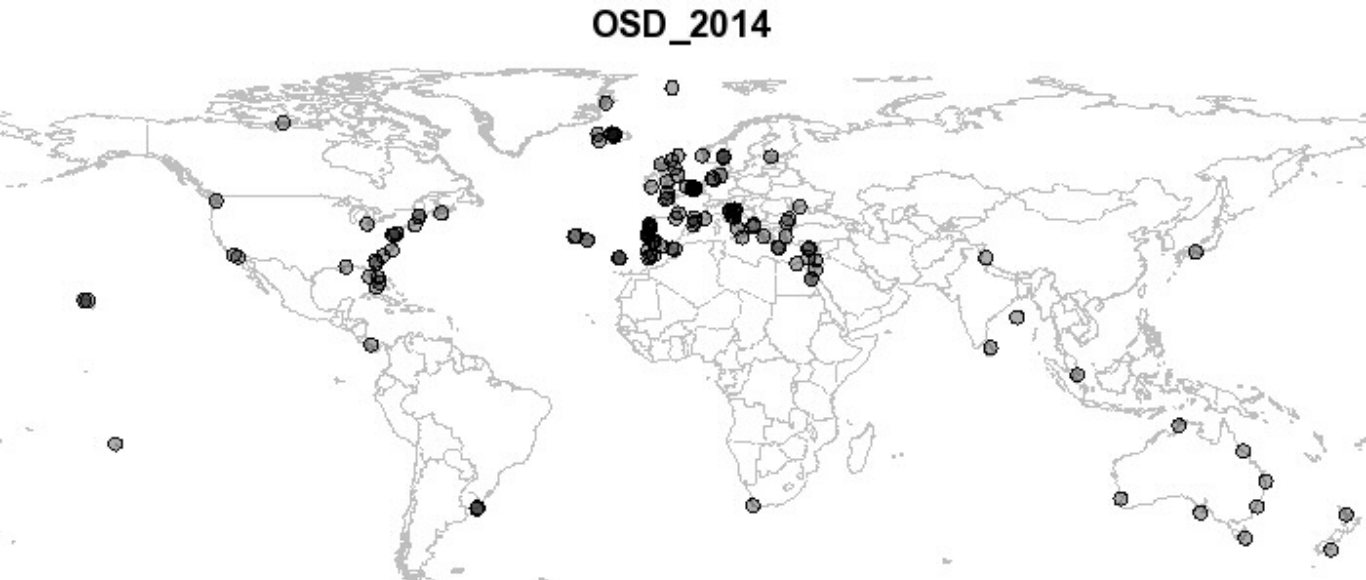

Suppl. Figure 3: The Ocean Sampling Day Campaign of 2014. Sampling stations are indicated by the grey dots on the map.

Supplementary materials 1: Bioinformatics details

Trimmomatic: parameters used.

java -jar trimmomatic.jar PE -threads 32 -phred33 -trimlog SkChyt5_trimming SkChyt5_S2_L002_R1_001.fastq SkChyt5_S2_L002_R2_001.fastq SkChyt5_paired1 SkChyt5_unpaired1 SkChyt5_paired2 SkChyt5_unpaired2 ILLUMINACLIP:FastQC_detected_IlluminAdapters.fasta:2:30:10 SLIDINGWINDOW:4:15 LEADING:3 TRAILING:3 MINLEN:36

Adapters detected by FastQC:

>TruSeq Adapter, Index 4 (100% over 50bp)

GATCGGAAGAGCACACGTCTGAACTCCAGTCACTGACCAATCTCGTATGC

>Illumina Single End PCR Primer 1 (100% over 50bp)

GATCGGAAGAGCGTCGTGTAGGGAAAGAGTGTAGATCTCGGTGGTCGCCG

Customised script to retrieve target genes from transcriptome/genome datasets

```
#!/bin/bash

#input: positional arguments:  1) assembled transcriptome or genome (.fasta), 2) seq(s) of gene(s) (.fasta) of interest to be searched in the genome/transcriptome

#usage example: ContigBlaster_V8.sh genome_transcriptome.fas query_seqs.fas

#step 1: Transform the genome in a BLAST database

for i in $1; do

BLASTDB=$(makeblastdb -in $i -dbtype nucl -title "$1-BLASTdb" -out "$1"bdb -parse_seqids)

Done


#step 2: search the gene(s) of interest in the genome and extract the names of the matching contigs and use them to retrieve their sequences.

#linearizes and shortens the name to produce a fasta as below:

#>CONTIG1_NAME

#sequence1atgtgtggttgagcgtagtcgatcgtatagct

#>CONTIG2_NAME

#sequence2atgcgcgctgctagtcgtagctagtcgtagct

#remove useless file and store BLASTdb in a single folder

#message: how many Hits your gene(s) have in the genome, i.e. how many contigs were retrieved by the gene.

for i in $2; do

SEARCHDB=$(blastn -db "$1"bdb -query $i -outfmt "10" > "$i"_bestHits.csv)

NAMEXTRACT=$(awk -F "\"*,\"*" '{print $2}' "$i"_bestHits.csv > "$i"_besthits_Ids)

SEQSEXTRACT=$(blastdbcmd -db "$1"bdb -dbtype nucl -entry_batch "$2"_besthits_Ids -outfmt %f -out "$2"_seqs.fasta)

LINEARIZE=$(sed -e 's/\(^>.*$\)/#\1#/' "$2"_seqs.fasta | tr -d "\r" | tr -d "\n" | sed -e 's/$/#/' | tr "#" "\n" | sed -e '/^$/d' > "$2"_blastres.fasta)

NAMESHORTENING=$(sed 's/len.*//g' "$2"_blastres.fasta > "$2"_contigs.fasta)

CLEANING=$(rm "$i"_bestHits.csv | rm "$i"_besthits_Ids | rm "$2"_seqs.fasta | rm "$2"_blastres.fasta)
```

```
ORGANIZEBDB=$(mkdir "$1"BLASTdb | mv "$1"bdb.* $1BLASTdb)

echo "$2 have $(grep -c '^>' "$2"_contigs.fasta) hits in $1"

done
```

#step 3: BLAST each retrieved contig against GenBank and gather the first 10 hits

#retrieves the corresponding accession numbers and the contig Id

```
for i in "$2"_contigs.fasta; do

BLASTNCBI=$(blastn -db nr -query $i -outfmt "10" -max_target_seqs 10 -perc_identity 98 -max_hsps 1 -remote > BLAST.csv)

ACCESSIONS=$(awk -F "\"*,\"*" '{print $2}' BLAST.csv > accessionumbers.txt)

done

echo "Accession numbers retrieved... looking for taxonomy"
```

#step 4: use the accession numbers to retrieve the taxonomy of the organism (according to GenBank).

#produces a .csv file containing the contig ID - 10 accessions and their taxonomy.

#removes useless files

```
echo "BLASTing $(grep -c '^>' "$2"_BLASTres.fasta) contigs"

for i in $(cat accessionumbers.txt); do

TAXLINAG=$(esearch -db nucleotide -query $i -sort id | efetch -db nucleotide -format fasta | awk -F '>' '{print $2}' | sed -n 1p| sed 's/,//g' >> GeneId.txt)

CONCATENATE=$(paste BLAST.csv GeneId.txt > BLASTtax.csv | sed 's/\t/,/g' BLASTtax.csv > BLAST_"$2"_contigs.csv)

done

CLEANING2=$(rm accessionumbers.txt | rm GeneId.txt | rm BLASTtax.csv | rm BLAST.csv)

echo "DONE! Output contains: retrieved contig sequences in "$2"_contigs.fasta + BLAST results for each contig in BLAST_"$2"_coontigs.csv"
```

Parameters used for the MOULINETTE script.

QUERY= SkChyt5_v4_rDNA.fasta

LIST= OSDlist.txt

PERCID= 97

MAXTARGET= 100

READCOVER= 0.8

EVALUE= 1e-130